Nonlinear Coherent Optical Systems in the Presence of Equalization Enhanced Phase Noise

Cenqin Jin, Nikita A. Shevchenko, Zhe Li, *Member, IEEE*, Sergei Popov, *Member, IEEE, Fellow, OSA*, Yunfei Chen, *Senior Member, IEEE*, and Tianhua Xu, *Member, IEEE*

***Abstract*—Equalization enhanced phase noise (EEPN) occurs due to the interplay between laser phase noise and electronic dispersion compensation (EDC) module. It degrades significantly the performance of uncompensated long-haul coherent optical fiber communication systems. In this work, a general expression accounting for EEPN is presented based on Gaussian noise model to evaluate the performance of multi-channel optical communication systems using EDC and digital nonlinearity compensation (NLC). The nonlinear interaction between the signal and the EEPN is analyzed. Numerical simulations are carried out in nonlinear Nyquist-spaced wavelength division multiplexing (WDM) coherent transmission systems. Significant performance degradation due to EEPN in the cases of EDC and NLC are observed, with and without the consideration of transceiver (TRx) noise. The validation of the analytical approach has been done via split-step Fourier simulations. The maximum transmission distance and the laser linewidth tolerance are also estimated to provide important insights into the impact of EEPN.**

***Index Terms*—Optical fiber communication, digital nonlinearity compensation, Gaussian noise model, laser phase noise, electronic dispersion compensation, equalization enhanced phase noise.**

I. Introduction

Recently, demands on high-capacity data transmission have drastically increased, especially since the outbreak of COVID-19. Optical fibers currently carry over about 95% of the global Internet traffic, and the ever-growing demand on capacity poses higher requirements for optical transmission systems. Nyquist-spaced transmission is implemented to enhance the spectral efficiencies (SEs), as well as optical signal distortions are strictly mitigated to ensure the sufficient signal quality. It has been reported that chromatic dispersion (CD), polarization mode dispersion (PMD), laser phase noise (LPN), and fiber nonlinear interference (NLI) due to optical Kerr effect, can be essentially suppressed by means of advanced digital signal processing (DSP) techniques [1], [2]. However, the interactions, which occur between LPN and CD, namely, equalization enhanced phase noise (EEPN), cannot be easily compensated [2], [3]. EEPN, arising from the interaction between LPN and electronic dispersion compensation (EDC) module in DSP-based coherent systems. The impact of EEPN usually scales with the fiber dispersion, the linewidth of the local oscillator (LO) or the transmitter (Tx) laser, the modulation format and the signal symbol rate [4], [5]. As it has been studied in [6]–[8], EEPN may significantly degrade the performance of optical fiber transmission systems. However, to the best of our knowledge, studies on EEPN so far have been only performed for the systems without considering any nonlinear interference (NLI). However, in modern long-haul optical fiber coherent transmission systems, the NLI caused by the optical Kerr effect in silica fibers cannot be neglected.

Analytical models have been used to evaluate the influence of NLI in coherent optical transmission systems. Among them, the family of Gaussian noise (GN) models (see, e.g., [9]–[11]) has become widely popular owing to its sufficiently accurate predictions and relatively low complexity. Latest GN models have also been developed for systems in the presence of transceiver (TRx) noise [12], [13]. However, no research has ever been reported on the GN model accounting for the EEPN. In addition to CD, LPN and NLI, the signal propagation in the fiber will be further distorted in the presence of EEPN. In such instance, theoretical predictions based on the conventional GN models may greatly overestimate the real system performance.

In this paper, we intend to investigate the impact of EEPN on nonlinear optical fiber transmission systems through split-step Fourier simulations and obtain accurate predictions of the system performance. Therefore, the GN model accounting for the impact of EEPN is described to predict the performance of long-haul Nyquist-spaced wavelength division multiplexing (WDM) coherent communication systems with both EDC and digital nonlinearity compensation (NLC). Both accuracy and effectiveness of our analytical approach were verified via split-step Fourier numerical simulations. The performance of single- and multi-channel systems with and without the EEPN were evaluated and compared. Our results indicate that EEPN can greatly degrade the system performance. The introduction of EEPN into the GN model is essential for an accurate performance evaluation of dispersion-unmanaged optical communication systems accounting for LPN from Tx and LO. Moreover, the maximum system reach for different laser linewidths and signal modulation formats is predicted and analyzed.

The rest of this paper is organized as follows: Section II introduces the principle of EEPN in optical fiber communication systems. Section III describes the analytical model for evaluating the impacts of amplifier noise, NLI and EEPN. Sec-

Manuscript received XXXX. This work is supported by EU Horizon 2020 MSCA-RISE Grant (No. 101008280) and Swedish Research Council (Vetenskapsrådet 2019-05197). (Corresponding author: Tianhua Xu) C. Jin, Y. Chen and T. Xu are with School of Engineering, University of Warwick, Coventry CV4 7AL, United Kingdom. T. Xu is also with Tianjin University, Tianjin 300072, China and University College London (UCL), London WC1E 6BT, United Kingdom (tianhua.xu@ieee.org). N. A. Shevchenko is with University of Cambridge, Cambridge CB3 0FA, United Kingdom (ms2688@cam.ac.uk). Z. Li is with II-VI Incorporated, Horsham, PA 19044, United States (zhe.li@ieee.org). S. Popov is with KTH Royal Institute of Technology, Stockholm 16440, Sweden (sergeip@kth.se).

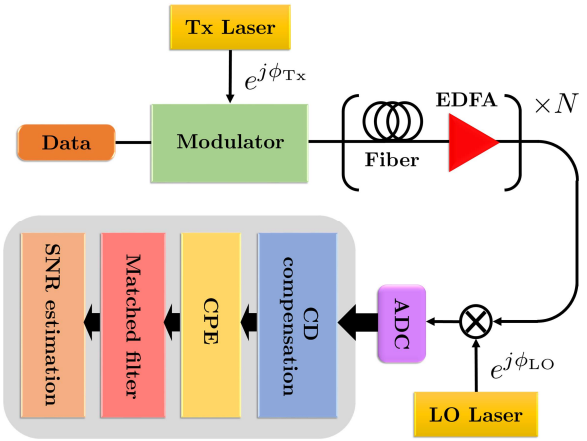

Fig. 1. Principle of EEPN in optical fiber communication system. EDFA: erbium-doped fiber amplifier. ADC: analog-to-digital converter. SNR: signal-to-noise ratio

tion IV presents the transmission setup. Results are discussed in Section V and Section VI with and without considering the effect of TRx noise. Section VII presents the results of the simulations considering PMD. Section VIII provides the conclusion.

II. Equalization-Enhanced Phase Noise

The EEPN effect originates from the non-zero net dispersion experienced by the Tx or the LO LPN [7], [14]. Fig. 1 illustrates the origin of EEPN in optical fiber communication systems. In a coherent optical transmission system without optical dispersion compensation (ODC), CD compensation and carrier phase estimation (CPE) are applied using DSP on the receiver (Rx) side. The matched filter is applied before the SNR estimation for selecting the observed channel. The Tx and the LO lasers provide phase fluctuations of $e^{j\phi_{\text{Tx}}}$ and $e^{j\phi_{\text{LO}}}$, respectively. The LPN from the Tx laser is firstly dispersed in the optical fiber and then experiences the CD compensation at the Rx. The net dispersion experienced by the Tx LPN is close to zero. However, the LPN from the LO laser passes through CD compensation only and will be severely dispersed. In this scenario, EEPN is generated due to the interaction between the CD compensation module and the LO LPN [6]. EEPN can also be produced from the interaction between fiber dispersion and the Tx LPN [14], [15]. However, the LO LPN induced EEPN is more common and all analyses in this paper are performed in this scenario.

The variance of EEPN is proportional to the accumulated CD, the 3-dB linewidth of the LO (or Tx) laser, and the transmission bandwidth and can be calculated as [7], [16]

$$\sigma^2_{\text{EEPN}}(L) = N\,\frac{\pi c\,D\,L\,f_{3\text{dB}}}{2f_0^2}\cdot R\,, \tag{1}$$

where N is the number of fiber spans in a link, c is the speed of light in vacuum, D is the chromatic dispersion coefficient, L is the fiber span length, $f_{3\text{dB}}$ is the 3-dB laser linewidth, and f_0 is the laser center frequency, R is the signal symbol rate.

III. Analytical Model

In this section, the analytical model is presented to predict the signal-to-noise ratio (SNR) in dispersion-unmanaged Nyquist-spaced coherent optical transmission systems in presence of EEPN, where the EDC and the NLC are applied respectively.

Considering such a transmission system, nonlinear distortions can be modeled as additive Gaussian noise, which is appropriate for signals distorted by moderate fiber nonlinearities and significant dispersion in long-haul transmission systems. The conventional GN model considers the distortion caused by NLI and amplified spontaneous emission (ASE) noise. It is given by the following expression [17], [18]

$$\text{SNR} = \frac{P}{P_{\text{ASE}} + P_{\text{NLI}} + P_{\text{Signal-ASE}}}\,, \tag{2}$$

where P is the optical launch power per channel, P_{ASE} is the ASE noise power arising from the erbium-doped optical fiber amplifier (EDFA), P_{NLI} is the signal-signal interaction caused by the optical Kerr effect, and $P_{\text{Signal-ASE}}$ is the signal-ASE interaction due to the four-wave mixing process. The dual polarization P_{ASE} is evaluated by the well-known expression $N\,(G\text{–}1)\,F_n\,hf_0\cdot R$, with the EDFA gain G, the EDFA noise figure F_n, and the Planck constant h. Considering a Nyquist-spaced system with multiple identical fiber spans, and accounting for the impact of input signal modulation format [19], the signal-signal NLI noise power at the central channel has the following closed-form approximation [20]

$$\begin{aligned} P_{\text{NLI}} &\triangleq \eta\,(N, N_{\text{ch}})\cdot P^3 \\ &\approx \frac{8}{27}\frac{\gamma^2 N L_{\text{eff}}}{\pi\,|\beta_2|\,R^2}\left\{N^{\varepsilon}\,\text{asinh}\left(\frac{\pi^2}{2}\,|\beta_2|\,L_{\text{eff}}\cdot N_{\text{ch}}^2\,R^2\right)\right. \\ &\quad \left. -\,\chi\,\frac{10}{3}\frac{L_{\text{eff}}}{L}\left[\text{HN}\left(\frac{N_{\text{ch}}-1}{2}\right)+1\right]\right\}\cdot P^3\,, \end{aligned} \tag{3}$$

where $\eta\,(N, N_{\text{ch}})$ is the NLI distortion coefficient, γ is the fiber nonlinear coefficient, L_{eff} is the effective fiber span length, β_2 is the group velocity dispersion parameter, ε is the so-called coherence factor [18], $\text{asinh}\,(\cdot)$ denotes the inverse hyperbolic sine, N_{ch} is the total number of channels in the system, χ denotes the constant, which depends on the signal modulation format, whose values for dual-polarisation quadrature phase shift keying (DP-QPSK), dual-polarization 16-ary quadrature amplitude modulation (DP-16QAM), DP-32QAM, DP-64QAM, and DP-Gaussian are equal to $\{1, 17/25, 69/100, 13/21, 0\}$, respectively; and $\text{HN}\,(x)$ stands for the harmonic number series, defined as follows $\sum_{n=1}^{x} 1/n$.

As mentioned in Section I, the conventional GN model would significantly overestimate the system performance, if the EEPN noise was not negligible. For more practical cases with considerable LPNs from Tx and Rx lasers, the EEPN contribution should be added in the estimation of SNR. Accounting for the EEPN effect, the updated expression of Eq. (2) is now given by

$$\text{SNR} = \frac{P}{P_{\text{ASE}} + P_{\text{NLI}} + P_{\text{Signal-ASE}} + \sigma^2_{\text{EEPN}}\cdot P}\,, \tag{4}$$

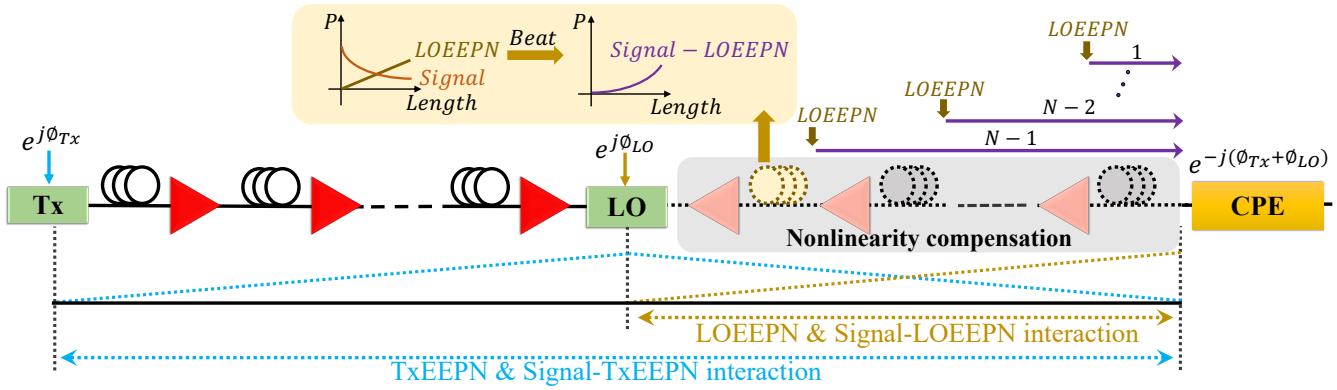

Fig. 2. Schematic of EEPN and Signal-EEPN interactions accumulation process in an optical communication system using NLC.

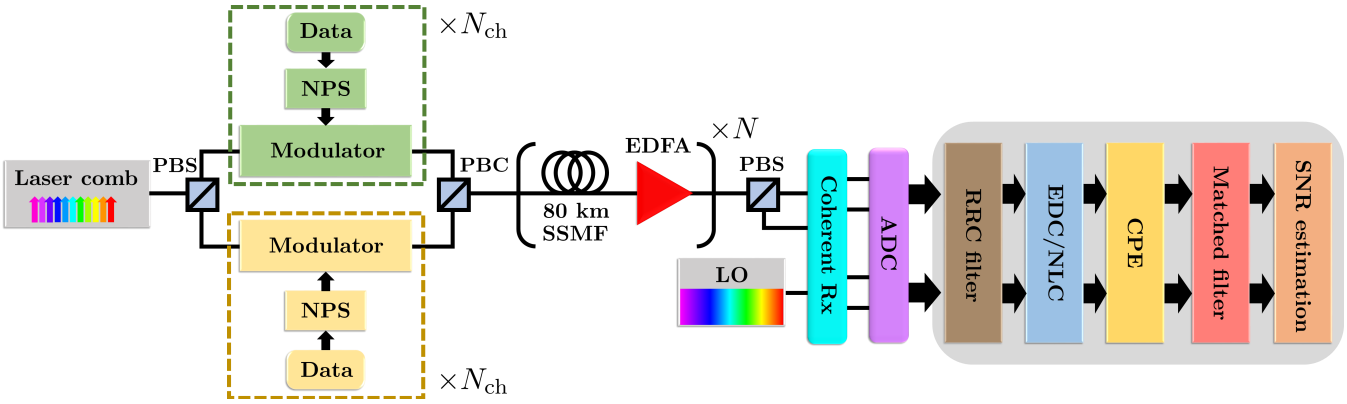

Fig. 3. Simulation setup of DP-16QAM Nyquist-spaced WDM transmission system using EDC or NLC. NPS: Nyquist pulse shaping; PBS: polarization beam splitter; PBC: polarization beam combiner.

where σ^2_{EEPN} is the variance of EEPN given by Eq. (1).

In the case of EDC, $P_{\text{Signal-ASE}}$ can be neglected as its contribution is much smaller than the P_{NLI}. When NLC is applied in the system, the signal-signal NLI P_{NLI} is greatly reduced. The signal-ASE interaction $P_{\text{Signal-ASE}}$, which is neglected in the EDC case, becomes relatively significant and needs to be considered. The NLC considered in this paper refers to the full-field compensation (i.e., applied to all signal bandwidths). Thus, the signal-signal NLI can be completely removed. The nonlinear interaction between the signals and EEPN effects should also be taken into account, as it happens when the signals pass through the NLC module. Fig. 2 shows the schematic of EEPN and EEPN-signal interactions accumulation process in an optical communication system using NLC. In presence of EEPN, the model expressions for the case of EDC and NLC are given respectively by

$$\text{SNR}_{\text{EDC}} = \frac{P}{P_{\text{ASE}} + P_{\text{NLI}} + \sigma^2_{\text{EEPN}} \cdot P}, \tag{5}$$

$$\text{SNR}_{\text{NLC}} = \frac{P}{P_{\text{ASE}} + P_{\text{Signal-ASE}} + \sigma^2_{\text{EEPN}} \cdot P + P_{\text{Signal-EEPN}}}, \tag{6}$$

where $P_{\text{Signal-ASE}}$ exhibits the quadratic growth with launch power, and can be estimated by the following expression $3\,\xi\,\eta\,(1, N_{\text{ch}})\,P_{\text{ASE}} \cdot P^2$ with the NLI distortion coefficient $\eta\,(1, N_{\text{ch}})$ evaluated after one span propagation, and the factor $\xi \triangleq \sum_{k=1}^{N} k^{\varepsilon+1}$ (see, e.g., [9], [10], [21]); $P_{\text{Signal-EEPN}}$ is the interaction between the signal and the EEPN effect due to the four-wave mixing process, and it is approximately estimated as $3\,\xi\,\eta\,(1, N_{\text{ch}})\,(\sigma^2_{\text{EEPN}}/N) \cdot P^3$. This expression gives rise to an overestimation of the noise variance due to the signal-EEPN interaction. More accurate evaluation of the signal-EEPN interaction can be found in Appendix A. It is worth noting that in the presence of NLC the amount of EEPN contribution is larger than that in the case of EDC. This happens due to the appearance of extra signal-EEPN interaction.

The optimum launch power for the EDC case can be obtained by setting the derivative of Eq. (5) to zero and solving the arising equation. Then we can obtain the maximum SNR by substituting the optimum launch power in Eq. (5). The optimum launch power and the corresponding maximum SNR in the case of EDC are expressed as

$$P_{\text{EDC,opt}} = \sqrt[3]{\frac{P_{\text{ASE}}}{2N^{\varepsilon}\,\eta\,(1, N_{\text{ch}})}}, \tag{7}$$

$$\max_{P}\left[\,\text{SNR}_{\text{EDC}}\,\right] = \frac{1}{\sigma^2_{\text{EEPN}} + \sqrt[3]{\frac{27}{4}N^{\varepsilon+3}\,\eta\,(1, N_{\text{ch}})\;P^2_{\text{ASE}}}}. \tag{8}$$

Similarly, the optimum launch power and the corresponding maximum SNR for the use of NLC are described as

$$P_{\text{NLC,opt}} \approx \sqrt{\frac{N}{3\xi\,\eta(1,N_{\text{ch}})}}\,, \tag{9}$$

$$\max_{P}\left[\,\text{SNR}_{\text{NLC}}\,\right] \approx \frac{1}{\sigma^2_{\text{EEPN}} + \sqrt{12\xi N\eta(1,N_{\text{ch}})P^2_{\text{ASE}}}}\,. \tag{10}$$

Here we provide simple and accurate predictions of the optimum launch power and the achievable maximum SNR for both the EDC and the NLC schemes when there exist considerable Tx and LO laser phase noise in long-haul optical fiber communication systems.

IV. Transmission System

Numerical simulations have been performed to assess the impact of the EEPN on the system performance. The simulation setup of a Nyquist-spaced 32-GBd DP-16QAM WDM optical transmission system is described in Fig. 3. At the Tx, a 32-GHz spaced laser comb is used as the source of the optical carrier. The symbol sequence of the transmitted signal in each channel is fully random and independent. A root-raised cosine (RRC) filter with 0.1% roll-off is employed for Nyquist pulse shaping (NPS). A recirculating fiber loop is used in the transmission link. Standard single mode fiber (SSMF) is employed with a span length of 80 km. The signal propagation over the optical fiber is simulated based on the split-step Fourier solution of the Manakov equation [22], [23]. After each span of fiber, an EDFA with a 4.5 dB noise figure is applied to exactly compensate for the loop loss. At the Rx, the signal is mixed with a LO laser for coherent detection. Two scenarios are considered: 1) LO linewidth of 100 kHz to analyse the impact of EEPN; 2) LO linewidth of 0 Hz as a benchmark for no EEPN applied in the system. The signals are detected by photo detectors and sampled by analog-to-digital converters (ADCs).

In DSP modules, a RRC filter is applied before the NLC (or EDC) module to select the NLC bandwidth. A frequency domain equalizer (FDE) is used as the EDC module [24]. The Rx-side NLC is applied based on the reverse split-step Fourier solution of Manakov equation [25]. An ideal CPE is used for the compensation of phase noise, achieved by using the conjugate multiplication between the received signal and the extracted intrinsic laser phase noise. This is to focus on the impact from EEPN, where no amplitude noise mitigation effect is employed in the CPE module [14]. The matched filter is used to select the observed (center) channel and remove the out-of-band noise, and it is again achieved by an RRC filter with a roll-off factor of 0.1%. Finally, the performance of the central channel is estimated in terms of the SNR. The laser frequency offset and PMD are neglected in the simulation. Detailed parameters of the transmission system are given in Table I.

TABLE I
System Parameters

Parameters	Values
Center wavelength [nm]	1550
Attenuation coefficient [dB/km]	0.2
CD coefficient (D) [ps/nm/km]	17
Nonlinear coefficient (γ) [1/W/km]	1.2
EDFA noise figure (F_n) [dB]	4.5
Total fiber length ($N \times L$) [km]	25×80
Symbol rate (R) [GBd]	32
Channel spacing [GHz]	32
Number of channels (N_{ch})	$\{1, 5, 9\}$
Modulation format	16QAM
Roll-off factor [%]	0.1
Number of symbols	2^{20}
LO laser linewidth [kHz]	$\{0, 100\}$

V. Results and Analyses

Numerical simulations and analytical model predictions have been carried out for the DP-16QAM system over a transmission distance of 2000 km (25 fiber spans). Fig. 4(a), Fig. 4(b) and Fig. 4(c) show the results for the cases of single-channel, 5-channel and 9-channel transmission, respectively. Lines represent predictions from the proposed model expression, and markers represent simulation results. It is observed that the simulation results are highly consistent with the model in both cases of EDC and NLC. From Fig. 4, it can also be found that the EEPN has an important impact on the performance of NLC. This shows that the EEPN variance is significantly smaller than the signal-signal interaction in Eq. (5) but is considerably large compared to the signal-ASE interaction in Eq. (6). For the NLC case, it is found that the SNR with EEPN is 2.09 dB lower than that without EEPN at the optimal power of 9 dBm for the single-channel system. Similarly, the gaps are 1.41 dB and 1.35 dB at 7 dBm for the 5-channel and the 9-channel transmission systems, respectively. Their constellations at the optimum powers (without and with EEPN) are also shown in the insets. It can be seen that the EEPN causes significant distortion to the signal constellations.

Fig. 5 shows the SNR (left side) and the noise power (right side) of the central channel as a function of transmission distance in the DP-16QAM 5-channel Nyquist-spaced system using NLC at a fixed launch power of 7 dBm, with and without the application of EEPN. It can be observed that the additional degradation of SNR caused by EEPN exceeds 1 dB for all considered transmission distances from 800 to 4000 km. The deviation in conventional GN model caused by neglecting the EEPN is significant. The noise power in the system is also presented in Fig. 5. Square markers indicate the total power of EEPN, NLI, and ASE noise generated in the transmission system with a LO laser linewidth of 100 kHz, while triangle markers represent the power of NLI and ASE noise for the ideal LO laser system (neglecting the LO linewidth). Therefore, the "gap" between these two markers indicates the power of EEPN, as shown in Fig. 5 (right side). Continuous growth of EEPN power can be observed with the increase of the transmission distance (from 0.14 mW at 800 km to 1.66 mW at 4000 km, a total increase of ~ 12 times).

Next, the maximum reach and the LPN tolerance in optical communication systems are discussed based on the analytical model. Calculated SNRs from Section III are converted to

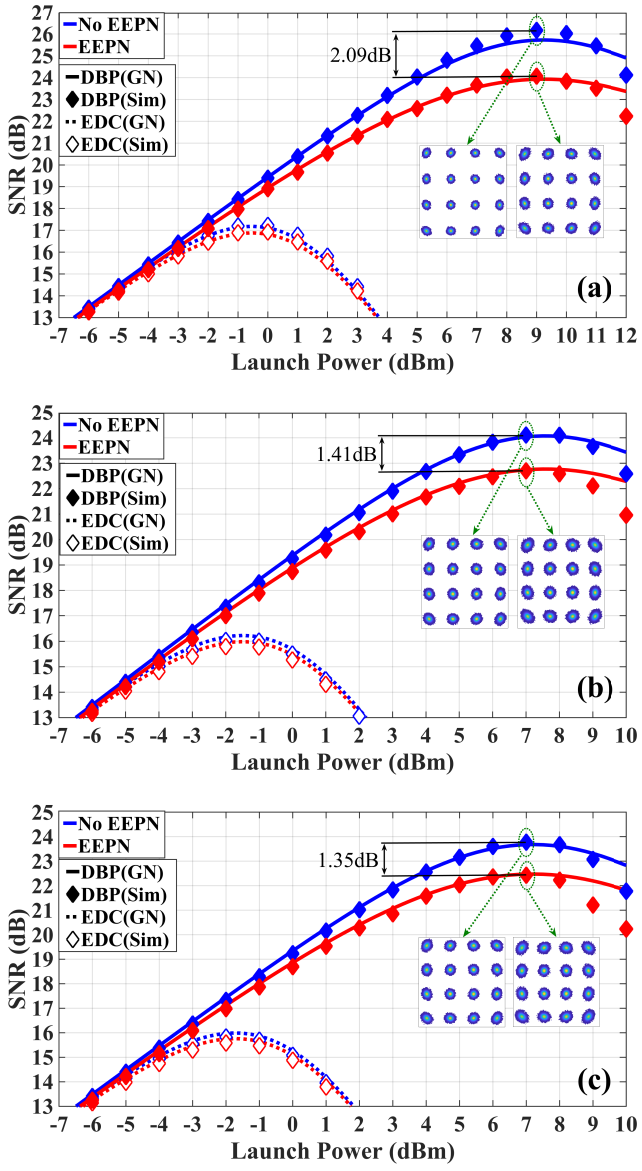

Fig. 4. The SNR of the central channel as a function of launch power per channel in the DP-16QAM Nyquist-spaced system with the single-channel transmission in (a), with the 5-channel transmission in (b), and with the 9-channel transmission in (c). The transmission distance is fixed at 2000 km. Lines represent the models, and markers represent simulation results. The EDC model Eq. (5) is shown with a dotted line, and the NLC model Eq. (6) is shown with a solid line. The constellations at the optimal simulation performance in the NLC systems are shown in the insets.

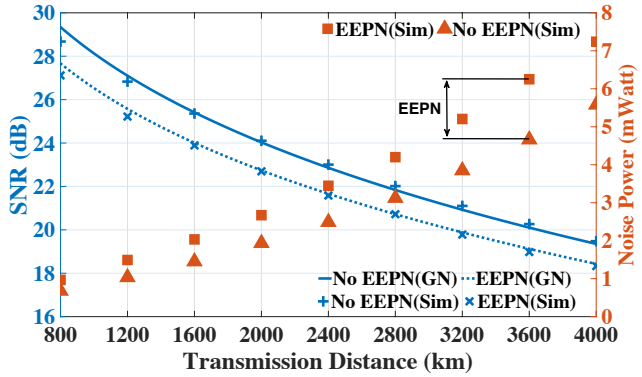

Fig. 5. The SNR (left side) and noise power (right side) of the central channel as a function of transmission distance in the DP-16QAM 5-channel Nyquist-spaced system at 7 dBm per channel launched power using NLC, with and without EEPN. Lines represent the model in Eq. (6), and markers represent results obtained by simulations.

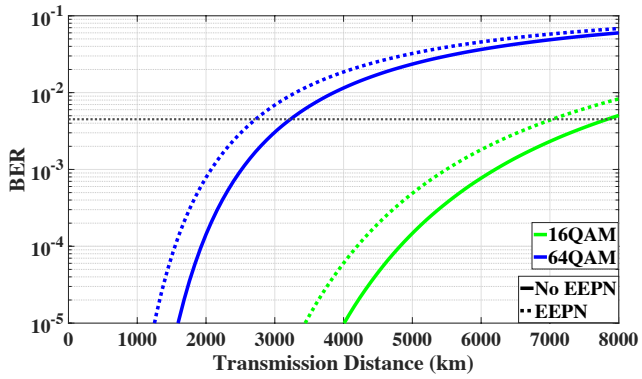

Fig. 6. The theoretical BER as a function of transmission distance in the 5-channel Nyquist-spaced system using NLC, with and without EEPN for the modulation format of 16QAM and 64QAM. The black dotted line indicates the FEC threshold (BER of 4.5×10^{-3}).

BERs for a clear analysis [24]. Modulation formats of DP-QPSK, DP-16QAM,and DP-64QAM are considered. Detailed parameters used for estimations, such as center wavelength, fiber parameters, symbol rate and EDFA noise figure etc. are the same as those listed in Table I. Fig. 6 shows the achievable BER as a function of transmission distance in the 5-channel Nyquist-spaced system using NLC, with and without EEPN (LO laser linewidth of 100 kHz and 0 Hz, respectively) for the modulation formats of 16QAM and 64QAM. The black dotted line indicates the BER threshold of 4.5×10^{-3}, corresponding to a 7% overhead hard-decision forward-error-correction (FEC) error-free threshold [26], which is applied to evaluate the system performance with a robust transmission margin. The length of each SSMF span is again 80 km. It is shown that the maximum transmission distance for 16QAM system considering EEPN is 6960 km, which is 800 km less than that of the system without EEPN. Similarly, the EEPN reduced the maximum reach by 480 km for the 64QAM system (from 3200 km to 2720 km). The QPSK result is not presented here, since it can support a transmission over 10000 km under the FEC threshold, even with the distortion from EEPN.

Fig. 7 shows the theoretical BER as a function of LO laser linewidth in the 5-channel Nyquist-spaced system using NLC for the modulation format of QPSK, 16QAM, and 64QAM. The black dotted line again indicates the BER threshold of 4.5×10^{-3}. Linewidths of typical lasers used in optical fiber communication systems, such as external cavity lasers (ECLs), and distributed feedback (DFB) lasers, are considered [27]. The transmission distance is fixed at 2000 km for Fig. 7(a) and 4000 km for Fig. 7(b). It can be seen from Fig. 7(a) that in order to ensure the transmission over a 2000 km fiber link, the LO laser linewidths in 16QAM and 64QAM systems need to be smaller than 2.032 MHz and 0.308 MHz, respectively. The BER of QPSK is well below the FEC threshold for any LO laser linewidth of from 0 to 5 MHz. From Fig. 7(b), it

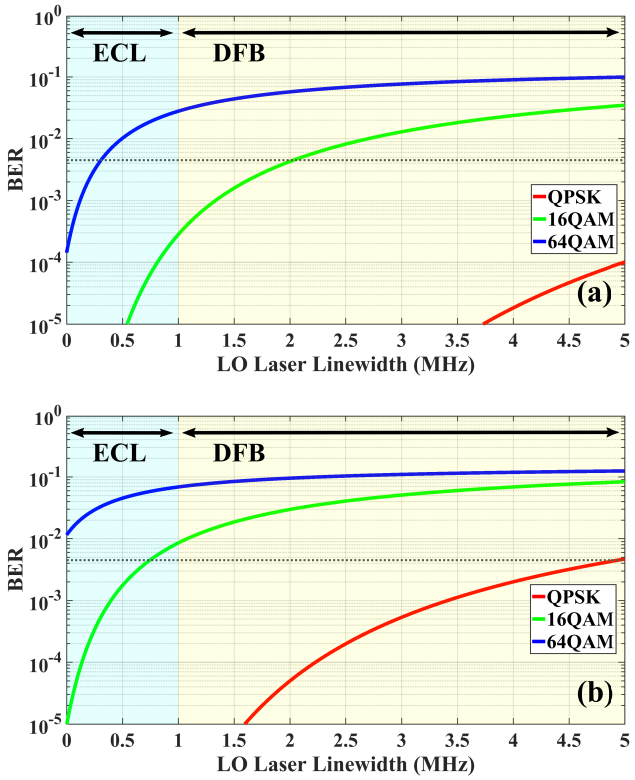

Fig. 7. The analytical BER as a function of LO laser linewidth in the 5-channel Nyquist-spaced system using NLC for the modulation format of QPSK, 16QAM, and 64QAM with transmission distance of 2000 km (a) and 4000 km (b). The black dotted line indicates the FEC threshold (BER of 4.5×10^{-3}).

can be observed that below the FEC threshold, the maximum allowable LO laser linewidth in 16QAM and QPSK systems with a transmission distance of 4000 km are 0.746 MHz and 4.944 MHz. The DP-64QAM system, even without the impact of EEPN, cannot meet the requirement of FEC at such a long distance. It is found that as the distance increases, the maximum LO linewidth of the system has to be decreased. This can also be observed in Fig. 8, which specifically shows the relationship between the maximum reach (under the 7% FEC threshold) and the LO linewidth. These lines are fitted by the 5th order polynomial. It can be observed from Fig. 8 that, when the LO linewidth is below 1 MHz, the maximum reach of 16QAM systems exceeds 3000 km, and 64QAM systems can transmit over 1000 km. When the LO linewidth is less than 2 MHz, the maximum reaches of 16QAM and 64QAM systems decrease dramatically. It tends to be stable when the LO linewidth is above 2 MHz. The QPSK systems with a LO linewidth of below 2 MHz can reach over 8000 km, and it can still transmit around 4000 km with a LO linewidth of 5 MHz.

VI. Impact of Transceiver Noise

The aforementioned analyses did not account for the impact of TRx noise, which includes all noise contributions from both the Tx and Rx, such as the finite resolution of digital-to-analog converters (DACs) and ADCs, the noise from the linear electrical amplifiers, and the noise from some optical components [13]. It defines the maximum achievable SNR in

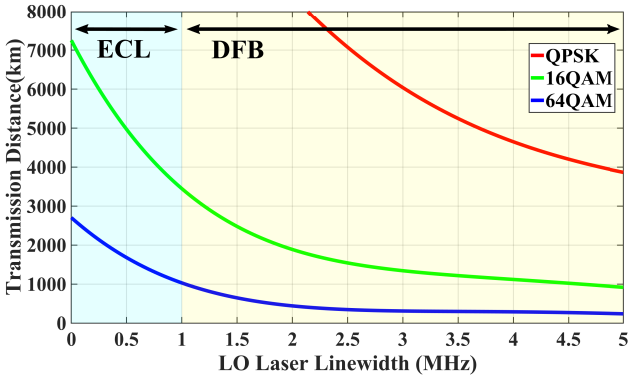

Fig. 8. The achievable transmission distance as a function of LO laser linewidth in the 5-channel Nyquist-spaced system using NLC for the modulation format of QPSK, 16QAM, and 64QAM under the FEC threshold (BER of 4.5×10^{-3}). The 5th order polynomial fit was applied.

a transmission system. In order to further assess the impact of the EEPN in practical systems, numerical simulations considering TRx noise have been conducted in a 2000 km DP-16QAM Nyquist-spaced system with applying NLC. Similar to Eq. (6), the SNR estimated for case of NLC considering the TRx noise can expressed as

$$\mathrm{SNR}_{\mathrm{NLC}}^{\mathrm{TRx}} = \frac{P}{P_{\mathrm{ASE}} + P_{\mathrm{Signal\text{-}ASE}} + \sigma_{\mathrm{EEPN}}^2 \cdot P + P_{\mathrm{Signal\text{-}EEPN}} + P_{\mathrm{TRx}}}, \quad (11)$$

where P_{TRx} represents the noise power owing to combination of the TRx noise and its interaction with the signal. P_{TRx} can be calculated as $\kappa P + 3\,\eta\,(1, N_{\mathrm{ch}})\; N^{\varepsilon+1}\,\kappa_{\mathrm{R}} \cdot P^3$ [12], where $\kappa \triangleq \mathrm{SNR}_{\mathrm{TRx}}^{-1}$, with the TRx SNR limit $\mathrm{SNR}_{\mathrm{TRx}}$ (the maximum achievable SNR in back-to-back systems); κ_{R} is the reciprocal of the receiver SNR limit, which is the maximum SNR considering noise from the Rx only. The TRx SNR limit was set to 25 dB in our simulation with an equal split of TRx noise between the Tx and Rx, where $\kappa_{\mathrm{R}} = \kappa/2$. This is a typical value for practical superchannel systems [12]. The transmission system has been presented in Section IV. Detailed settings were as the same as those in Table I.

The results are shown in Fig. 9(a) and Fig. 9(b) for the single- and 5-channel DP-16QAM transmission systems, respectively. Excellent agreement between analytical predictions and simulation results can be attained. The gaps between the SNR with and without EEPN are also very significant. EEPN caused reductions in the SNRs, $\sim$ 0.83 dB in the single-channel system and $\sim$ 0.76 dB in the 5-channel system. Simulation results demonstrate that the system performance degradation due to EEPN is still significant under the influence of TRx noise. Therefore, when evaluating the performance of optical communication systems with LPN, it is necessary to account for the impact of the EEPN effect.

VII. Impact of Polarization Mode Dispersion

The PMD effect was neglected in previous simulations. In order to further assess the impact of the EEPN in practical systems, numerical simulations considering PMD have also

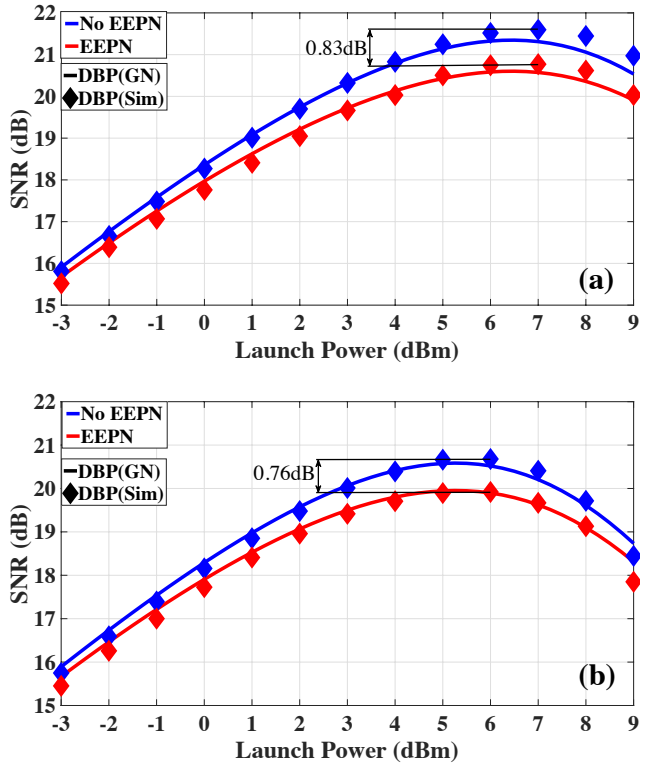

Fig. 9. The SNR of the central channel as a function of launch power per channel in the single-channel (a) and 5-channel (b) DP-16QAM Nyquist-spaced system with 25 dB TRx noise. The transmission distance is fixed at 2000 km. Lines represent the models, and markers represent simulation results.

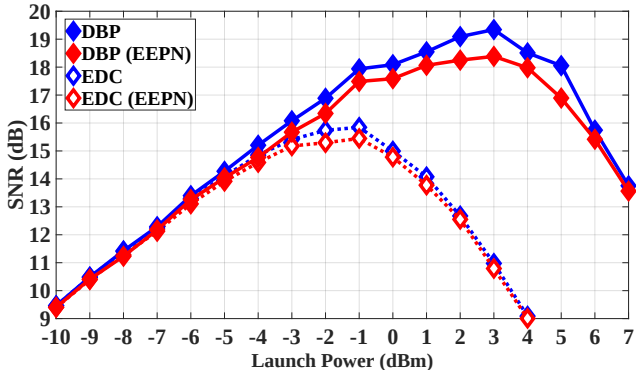

Fig. 10. The average SNR of the central channel as a function of launch power per channel in the 5-channel DP-16QAM Nyquist-spaced system in the presence of PMD. The transmission distance is fixed at 2000 km.

been conducted in a 2000 km 5-channel DP-16QAM Nyquist-spaced system with applying NLC and EDC. The signal propagation was simulated by solving the Manakov-PMD equation [22]. The PMD parameter in the system was set as 0.1 $\mathrm{ps}/\sqrt{\mathrm{km}}$. The simulation setup is similar with that described in Fig. 3. In order for mitigating the PMD effect, we additionally applied a blind multiple modulus algorithm (MMA) equalizer [28] after the matched filter. Other simulation details of the transmission setup are the same as those listed in Table I.

Simulation results are shown in Fig. 10. Despite that in the presence of PMD the performance of EDC case degrades marginally [29], [30], and NLC performance degrades considerably, the gaps between the SNRs with and without EEPN still remain significant. EEPN caused the SNR reductions of $\sim$ 1 dB in case of NLC, and $\sim$ 0.45 dB in case of EDC. Simulation results indicate that the system performance degradation due to EEPN remains substantial even in the presence of PMD effect.

VIII. Conclusion

An analytical model accounting for the impact of EEPN was presented for evaluating the performance of nonlinear Nyquist-spaced optical communication systems. The significance of EEPN contribution in nonlinear optical transmission systems as well as the accuracy and effectiveness of the analytical approach were validated via split-step Fourier numerical simulations. In the case of NLC, an SNR reduction of 1.41 dB in a 5-channel system due to EEPN was observed. Furthermore, it remained significant when a practical TRx limit noise and PMD are considered. Simulation results also showed a substantial growth of the EEPN impact with increasing the transmission distance.

Our work extends the scope of conventional GN model applications and demonstrates the relevance and importance of including the contribution of EEPN effect in the design and performance assessment of long-haul high-capacity optical communication systems with considerable laser linewidths.

Appendix A
Estimation of the Signal-EEPN Interaction

Corresponding power spectral densities (PSDs) for signal and noise contributions at Nyquist rate can be respectively defined as follows

$$S(f) \triangleq \frac{P}{R}\,\mathrm{rect}\left(\frac{f}{\mathrm{BW}}\right), \tag{12}$$

$$\begin{aligned} N_{\mathrm{EEPN}}(f\,|\,z) &\triangleq \frac{\sigma^2_{\mathrm{Signal-EEPN}}(z)\,P}{R}\,\mathrm{rect}\left(\frac{f}{\mathrm{BW}}\right) \\ &\equiv \sigma^2_{\mathrm{Signal-EEPN}}(z)\cdot S(f). \end{aligned} \tag{13}$$

where BW denotes the total WDM bandwidth, z is the transmission distance, $\sigma^2_{\mathrm{Signal-EEPN}}(z)$ is the variance of the signal-EEPN interaction.

Taking the transmission distance dependency of the EEPN variance in Eq. (13) into account gives rise to the following modifications in the GN-model based expressions

$$P_{\mathrm{Signal-EEPN}} \approx 3\,\xi\,\kappa\,\eta_{\mathrm{Signal-EEPN}}\cdot P^3, \tag{14}$$

where the nonlinear interference coefficient after one fiber span propagation is evaluated at the centre channel, it yields

$$\begin{aligned} \eta_{\mathrm{Signal-EEPN}} = \frac{16\,\gamma^2}{27R^2} &\int_{-\mathrm{BW}/2}^{\mathrm{BW}/2}\int_{-\mathrm{BW}/2}^{\mathrm{BW}/2} df_1\,df_2 \\ &\cdot \rho_{\mathrm{EEPN}}(f_1,f_2,0\,|\,L)\,\mathrm{rect}\left(\frac{f_1+f_2}{\mathrm{BW}}\right), \end{aligned} \tag{15}$$

where the FWM efficiency is now being defined as follows

$$\rho_{\,\mathrm{S-EEPN}}\left(f_1,f_2,0\,|\,L\right)=\int_0^L dz\,z\,e^{-\alpha z}\,e^{i\,\Delta\beta(0,f_1,f_2)\,z}$$

$$=\frac{1-\left[1+\left(\alpha-\,i\,\Delta\beta\left(0,f_1,f_2\right)\right)L\right]\cdot e^{-\left(\alpha-i\,\Delta\beta(0,f_1,f_2)\right)L}}{\left(\alpha-i\,\Delta\beta\left(0,f_1,f_2\right)\right)^2}\,, \tag{16}$$

where α is the attenuation coefficient, and the FWM mismatch factor $\Delta\beta\left(f,f_1,f_2\right)\;\approx\;4\pi^2[\,\beta_2+\pi\left(f_1+f_2\right)\beta_3\,]\cdot\left(f_1-f\right)\left(f_2-f\right)$, with β_2 and β_3 being the 2^{nd} and 3^{rd}-order dispersion coefficients. In Eq. (14), we have also introduced the following notation

$$\kappa\triangleq\frac{\sigma^2_{\mathrm{EEPN}}\left(L\right)}{N\cdot L}=\frac{\pi c\,D\,f_{3\mathrm{dB}}\,R}{2f_0^2}\,.$$

It is rather evident that a more accurate analysis of signal-EEPN interaction becomes more complicated, whilst it has been observed that the amount of signal-EEPN interaction itself remains marginal compared to other contributions in the reference SNR equation Eq. (6). Therefore, we used a simpler approach in the model, which essentially overestimates the impact of signal-EEPN interaction as described in the main text.

REFERENCES

[1] S. J. Savory, "Digital filters for coherent optical receivers," *Opt. Express*, vol. 16, no. 2, pp. 804–817, Jan. 2008.

[2] G. P. Agrawal, *Nonlinear Fiber Optics*. New York, USA: Academic Press, 2013.

[3] A. P. T. Lau, T. S. R. Shen, W. Shieh, and K.-p. Ho, "Equalization-enhanced phase noise for 100 Gb/s transmission and beyond with coherent detection," *Opt. Express*, vol. 18, no. 16, pp. 17 239–17 251, Aug. 2010.

[4] K.-P. Ho, A. P. T. Lau, and W. Shieh, "Equalization-enhanced phase noise induced timing jitter," *Opt. Lett.*, vol. 36, no. 4, pp. 585–587, Feb. 2011.

[5] K.-P. Ho and W. Shieh, "Equalization-enhanced phase noise in mode-division multiplexed systems," *J. Lightw. Technol.*, vol. 31, no. 13, pp. 2237–2243, Jul. 2013.

[6] A. Kakkar, J. R. Navarro, R. Schatz, H. Louchet, X. Pang, O. Ozolins, G. Jacobsen, and S. Popov, "Comprehensive study of equalization-enhanced phase noise in coherent optical systems," *J. Lightw. Technol.*, vol. 33, no. 23, pp. 4834–4841, Dec. 2015.

[7] W. Shieh and K.-P. Ho, "Equalization-enhanced phase noise for coherent-detection systems using electronic digital signal processing," *Opt. Express*, vol. 16, no. 20, p. 15718, Sept. 2008.

[8] T. Xu, G. Jacobsen, S. Popov, J. Li, S. Sergeyev, A. T. Friberg, T. Liu, and Y. Zhang, "Analysis of chromatic dispersion compensation and carrier phase recovery in long-haul optical transmission system influenced by equalization enhanced phase noise," *Optik*, vol. 138, pp. 494–508, Jun. 2017.

[9] P. Poggiolini, G. Bosco, A. Carena, V. Curri, Y. Jiang, and F. Forghieri, "The GN-Model of fiber non-linear propagation and its applications," *J. Lightw. Technol.*, vol. 32, no. 4, pp. 694–721, Feb. 2014.

[10] P. Poggiolini and Y. Jiang, "Recent advances in the modeling of the impact of nonlinear fiber propagation effects on uncompensated coherent transmission systems," *J. Lightw. Technol.*, vol. 35, no. 3, pp. 458–480, Feb. 2017.

[11] P. Poggiolini, Y. Jiang, A. Carena, and F. Forghieri, *Enabling Technologies for High Spectral-efficiency Coherent Optical Communication Networks (Chapter 7)*. US: Wiley, 2016.

[12] L. Galdino, D. Semrau, D. Lavery, G. Saavedra, C. B. Czegledi, E. Agrell, R. I. Killey, and P. Bayvel, "On the limits of digital back-propagation in the presence of transceiver noise," *Opt. Express*, vol. 25, no. 4, pp. 4564–4578, Feb. 2017.

[13] D. Semrau, L. Galdino, R. I. Killey, and P. Bayvel, "The impact of transceiver noise on digital nonlinearity compensation," *J. Lightw. Technol.*, vol. 36, no. 3, pp. 695–702, Feb. 2018.

[14] T. Xu, G. Liga, D. Lavery, B. C. Thomsen, S. J. Savory, R. I. Killey, and P. Bayvel, "Equalization enhanced phase noise in Nyquist-spaced superchannel transmission systems using multi-channel digital back-propagation," *Sci. Rep.*, vol. 5, p. 13990, Sept. 2015.

[15] G. Jacobsen, M. Lidón, T. Xu, S. Popov, A. T. Friberg, and Y. Zhang, "Influence of pre- and post-compensation of chromatic dispersion on equalization enhanced phase noise in coherent multilevel systems," *J. Opt. Commun.*, vol. 32, no. 4, pp. 257–261, Dec. 2011.

[16] A. Arnould and A. Ghazisaeidi, "Equalization enhanced phase noise in coherent receivers: DSP-aware analysis and shaped constellations," *J. Lightw. Technol.*, vol. 37, no. 20, pp. 5282–5290, Oct. 2019.

[17] P. Poggiolini, A. Carena, V. Curri, G. Bosco, and F. Forghieri, "Analytical modeling of nonlinear propagation in uncompensated optical transmission links," *IEEE Photonics Technol. Lett.*, vol. 23, no. 11, pp. 742–744, Jun. 2011.

[18] P. Poggiolini, "The GN Model of non-linear propagation in uncompensated coherent optical systems," *J. Lightw. Technol.*, vol. 30, no. 24, pp. 3857–3879, Dec. 2012.

[19] A. Carena, G. Bosco, V. Curri, Y. Jiang, P. Poggiolini, and F. Forghieri, "EGN model of non-linear fiber propagation," *Opt. Express*, vol. 22, no. 13, pp. 16 335–16 362, Jun. 2014.

[20] P. Poggiolini, G. Bosco, A. Carena, V. Curri, Y. Jiang, and F. Forghieri, "A simple and effective closed-form GN model correction formula accounting for signal non-Gaussian distribution," *J. Lightw. Technol.*, vol. 33, no. 2, pp. 459–473, 2015.

[21] T. Xu, N. A. Shevchenko, D. Lavery, D. Semrau, G. Liga, A. Alvarado, R. I. Killey, and P. Bayvel, "Modulation format dependence of digital nonlinearity compensation performance in optical fibre communication systems," *Opt. Express*, vol. 25, no. 4, pp. 3311–3326, Feb. 2017.

[22] D. Marcuse, C. R. Manyuk, and P. K. A. Wai, "Application of the Manakov-PMD equation to studies of signal propagation in optical fibers with randomly varying birefringence," *J. Lightw. Technol.*, vol. 15, no. 9, pp. 1735–1746, Sept. 1997.

[23] G. Bosco, A. Carena, V. Curri, R. Gaudino, P. Poggiolini, and S. Benedetto, "Suppression of spurious tones induced by the split-step method in fiber systems simulation," *IEEE Photonics Technol. Lett.*, vol. 12, no. 5, pp. 489–491, May 2000.

[24] G. P. Agrawal, *Fiber-optic communication systems*, 3rd ed. Hoboken, NJ, USA: Wiley, 2012.

[25] E. Ip and J. M. Kahn, "Compensation of dispersion and nonlinear impairments using digital backpropagation," *J. Lightw. Technol.*, vol. 26, no. 20, pp. 3416–3425, Oct. 2008.

[26] F. Chang, K. Onohara, and T. Mizuochi, "Forward error correction for 100 G transport networks," *IEEE Commun. Mag.*, vol. 48, no. 3, pp. S48–S55, Mar. 2010.

[27] ECL, DFB, VHG-Stabilized, DBR, and Hybrid Single-Frequency Lasers. Accessed 13-August-2020. [Online]. Available: {https://www.thorlabs.com/newgrouppage9.cfm?objectgroup_id=4737}

[28] M. P. Paskov, "Algorithms and subsystems for next generation optical networks," Ph.D. dissertation, University College London, London, UK, 2015.

[29] C. B. Czegledi, G. Liga, D. Lavery, M. Karlsson, E. Agrell, S. J. Savory, and P. Bayvel, "Polarization-mode dispersion aware digital back-propagation," in *ECOC 2016; 42nd European Conference on Optical Communication*. VDE, 2016, pp. 1–3.

[30] C. B. Czegledi, G. Liga, D. Lavery, M. Karlsson, E. Agrell, S. J. Savory, and P. Bayvel, "Digital backpropagation accounting for polarization-mode dispersion," *Opt. Express*, vol. 25, no. 3, pp. 1903–1915, 2017.